

Frequency-dependent reflection of elastic wave from thin bed in porous media

Hong-Xing Li(李红星), Chun-Hui Tao(陶春辉), Cai Liu(刘财), Guang-Nan Huang(黄光南), Zhen-An Yao(姚振岸)

Citation: Chin. Phys. B . 2020, 29(6): 064301 . **doi:** 10.1088/1674-1056/ab888b
Journal homepage: http://cpb.iphy.ac.cn; http://iopscience.iop.org/cpb

What follows is a list of articles you may be interested in

Micro-crack detection of nonlinear Lamb wave propagation in three-dimensional plates with mixed-frequency excitation

Wei-Guang Zhu(祝伟光), Yi-Feng Li(李义丰), Li-Qiang Guan(关立强), Xi-Li Wan(万夕里), Hui-Yang Yu(余辉洋), Xiao-Zhou Liu(刘晓宙)

Chin. Phys. B . 2020, 29(1): 014302 . **doi:** 10.1088/1674-1056/ab5931

Reflected and transmitted powers of arbitrarily polarized plane waves at interface between chiral and achiral media

Yan-Feng Lu(路彦峰), Yi-Ping Han(韩一平)

Chin. Phys. B . 2019, 28(2): 024202 . **doi:** 10.1088/1674-1056/28/2/024202

Seismoelectric wave propagation modeling in a borehole in water-saturated porous medium having an electrochemical interface

Hao-Ran Ding(丁浩然), Jin-Xia Liu(刘金霞), Zhi-Wen Cui(崔志文), Tribikram Kundu

Chin. Phys. B . 2017, 26(12): 124301 . **doi:** 10.1088/1674-1056/26/12/124301

Seismoelectric waves in a borehole excited by an external explosive source

Zhou Jiu-Guang, Cui Zhi-Wen, Lü Wei-Guo, Zhang Yu-Jun, Wang Ke-Xie

Chin. Phys. B . 2014, 23(1): 014301 . **doi:** 10.1088/1674-1056/23/1/014301

Frequency-dependent reflection of elastic wave from thin bed in porous media*

Hong-Xing Li(李红星)[1], Chun-Hui Tao(陶春辉)[2,3,†], Cai Liu(刘财)[4], Guang-Nan Huang(黄光南)[1], and Zhen-An Yao(姚振岸)[1]

[1] State Key Laboratory of Nuclear Resources and Environment, East China University of Technology, Nanchang 330013, China
[2] Key Laboratory of Submarine Geosciences, Second Institute of Oceanography, Ministry of Natural Resources, Hangzhou 310012, China
[3] School of Oceanography, Shanghai Jiao Tong University, Shanghai 200240, China
[4] Department of Geophysics, Jilin University, Changchun 130026, China

(Received 15 January 2020; revised manuscript received 31 March 2020; accepted manuscript online 12 April 2020)

The reflection of elastic wave from thin bed in porous media is important for oil and gas reservoir seismic exploration. The equations for calculating frequency-dependent reflection amplitude *versus* incident angle (FDAVA) from thin bed in porous media are obtained based on porous media theory. Some conclusions are obtained from numerical analysis, specifically, slow compression wave may be ignored when considering boundary conditions in most situations; the dispersion of reflection from thin bed is much higher than that from thick layer and is periodic in frequency domain, which is affected by the thickness of thin bed, velocity, and incident angle; the reflection amplitude envelope in frequency domain decays exponentially, which is affected by the thickness of thin bed, attenuation, and incident angle; the reflection amplitude increases with thickness of thin bed increasing, and then it decreases when the thickness reaches to a quarter of wavelength.

Keywords: frequency-dependent reflection, porous media, thin bed, reservoir

PACS: 43.20.Gp, 43.20.El, 82.33.Ln **DOI:** 10.1088/1674-1056/ab888b

1. Introduction

The reflection seismic survey is the most important method in the field of oil and gas reservoir exploration. The amplitude of seismic reflection wave carries the information about underground media. The reflection amplitude *versus* incident angle (AVA) can be used to predict hydrocarbon. The AVA from thin bed (including interbed) is one of the difficult points for reservoir prospection and prediction. The reflection from thin bed, calculated by Zeoppritz equation which is based on single phase elastic medium theory, was extensively studied.[1–7] But the oil and gas reservoir is typical of porous media. The theory of wave propagation in porous media has been adopted in the field of soil, ocean sediment, and oil–gas reservoir, and so on.[8–25] There are fast compressional wave (FP wave), slow compressional wave (SP wave) and conversed shear wave (CS wave) in porous media and the reflection at the interface of thick layer in porous media have been extensively studied.[26–29] The fluid flows in pores will bring about wave attenuation and dispersion, and the wave dispersion in a seismic frequency range is proved in porous media.[30,31] Frequency-dependent reflection amplitude *versus* incident angle (FDAVA) was developed in recent ten years.[32–38] But there has been no paper to describe the frequency-dependent reflection from thin bed based on porous medium theory. In this paper, the Biot/Squirt model (BISQ) of porous medium is reviewed first. Then, the equations for calculating the frequency-dependent reflection coefficient from thin bed based on porous medium are obtained. The frequency-dependent reflection coefficients *versus* incident angle from thin sandstone reservoir and alternating thin bed of sandstone and mudstone are calculated and analyzed to answer the questions about the effect of wave dispersion, the thickness and structure of thin bed on wave reflection.

2. Biot/Squirt theory

The BISQ equations of wave propagation can be expressed as follows:[16]

$$\begin{cases} \mu\nabla^2\boldsymbol{u}+(\lambda+\mu)\nabla(\nabla\cdot\boldsymbol{u})-\beta\nabla P=\dfrac{\partial^2}{\partial t^2}(\rho_1\boldsymbol{u}+\rho_2\boldsymbol{U}), \\ -\phi\nabla P=\dfrac{\partial^2}{\partial^2 t}(\rho_{11}\boldsymbol{u}+\rho_{22}\boldsymbol{U})-b\dfrac{\partial}{\partial t}(\boldsymbol{u}-\boldsymbol{U}), \end{cases} \tag{1}$$

$$P=-FS\left[\nabla\cdot\boldsymbol{U}+\frac{\beta-\phi}{\phi}\nabla\cdot\boldsymbol{u}\right], \tag{2}$$

where

$$F=\left(\frac{1}{K_{\rm f}}+\frac{\beta-\phi}{\phi}\frac{1}{K_{\rm s}}\right)^{-1}, \tag{3}$$

$$S=1-\frac{2{\rm J}_1(\lambda_1 r)}{\lambda_1 r{\rm J}_0(\lambda_1 r)}, \tag{4}$$

$$\lambda_1^2=\frac{\rho_{\rm f}\omega^2}{F}\left(\frac{\phi+\rho_{\rm s}/\rho_{\rm f}}{\phi}\right)+{\rm i}\frac{\eta\phi}{\kappa\rho_{\rm f}\omega}, \tag{5}$$

*Project supported by the National Natural Science Foundation of China (Grant Nos. 41764006, 41364004, and 41504095), the Chinese Study Abroad Fund (Grant No. 201508360117), the National Key Research and Development Program of China (Grant No. 2018YFC0309901), and the COMRA Major Project, China (Grant No. DY135-S1-01-01).

†Corresponding author. E-mail: taochunhuimail@163.com

© 2020 Chinese Physical Society and IOP Publishing Ltd

λ and μ being the elastic modulus of drained skeleton, β the pore-elastic coefficient, $b = \eta\phi^2/\kappa$ the dissipation coefficient, $\boldsymbol{u}$ the displacement vector of solid, $\boldsymbol{U}$ the displacement vector of fluid, P the fluid pressure, $\rho_1 = (1-\phi)\rho_s$, $\rho_2 = \phi\rho_f$, $\rho_{12} = -\rho_a$, $\rho_{11} = \rho_1 + \rho_{12}$, $\rho_{22} = \rho_2 + \rho_{12}$, ρ_s is solid density, ρ_f is fluid density, ρ_a is coupling density, κ the permeability, η the viscosity, K_s the bulk modulus of grains, K_f the bulk modulus of fluid, ω the angular frequency, r the Squirt length, ϕ the porosity, J_0 and J_1 the zero-order and first-order Bessel functions, respectively, ∇ the gradient operator, $\nabla\cdot$ the divergence operator, ∇^2 the Laplace operator, i the imaginary part of a complex number.

3. FDAVA theory of thin bed in porous media

The geological thin reservoir model is shown in Fig. 1(a). The medium I is the covering mudstone and the medium III is the under mudstone. The medium II is the thin reservoir which is single thin sandstone or thin sandstone and mudstone interbed. The incident FP wave will introduce the reflected FP wave, SP wave, CS wave into medium I and transmitted FP wave, and the SP wave and CS wave into medium III. There are up-going and down-going FP wave, SP wave, and CS wave in medium II (Fig. 1). The frequency, velocity, attenuation, thickness, and structure of thin bed all affect the FDAVA response from thin reservoir. For better comparisons, figure 1(b) shows thick layer model.

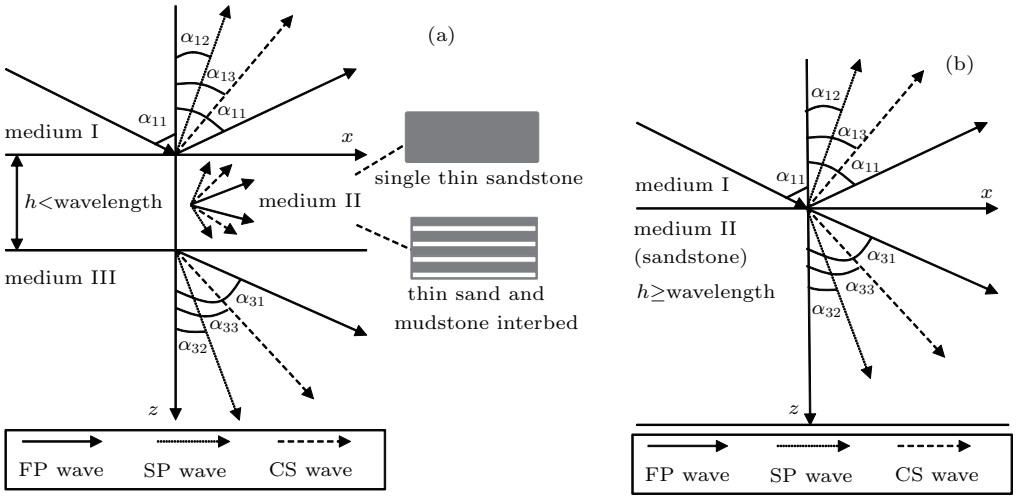


Fig. 1. Reflection and transmission from (a) thin bed and (b) thick layer based on BISQ theory.

The boundary conditions of reflection and transmission can be expressed by $u_z^1 = u_z^2\big|_{z=0}$, $u_x^1 = u_x^2\big|_{z=0}$, $\sigma_{zz}^1 = \sigma_{zz}^2\big|_{z=0}$, $\sigma_{xz}^1 = \sigma_{xz}^2\big|_{z=0}$, $P_1 = P_2\big|_{z=0}$, $\phi_1\left(u_z^1 - U_z^1\right) = \phi_2\left(u_z^2 - U_z^2\right)\big|_{z=0}$, $u_z^2 = u_z^3\big|_{z=h}$, $u_x^2 = u_x^3\big|_{z=h}$, $\sigma_{zz}^2 = \sigma_{zz}^3\big|_{z=h}$, $\sigma_{xz}^2 = \sigma_{xz}^3\big|_{z=h}$, $P_2 = P_3\big|_{z=h}$, $\phi_2\left(u_z^2 - U_z^2\right) = \phi_3\left(u_z^3 - U_z^3\right)\big|_{z=h}$, u_x and u_z are the displacement components of solid. U_x and U_z the displacement components of fluid, σ_{xx}, σ_{xz}, and σ_{zz} the stress components, superscripts 1, 2, and 3 refer to medium I, medium II, and medium III, respectively, subscript x means the horizontal direction, z the vertical direction. P_1, P_2, and P_3 are the fluid pressures in medium I, medium II, and medium III, respectively, ϕ_1, ϕ_2, and ϕ_3 the porosities in medium I, medium II, and medium III, respectively, and h is the thickness of thin bed. Then, the FDAVA equations of a single thin bed in porous media can be obtained by

$$\left[\boldsymbol{B}\boldsymbol{D}_1 \ -\boldsymbol{D}_2\right]\boldsymbol{R}_T = 0, \tag{6}$$

$$\boldsymbol{B} = \boldsymbol{M}\boldsymbol{W}\boldsymbol{M}^{-1}, \tag{7}$$

$$\boldsymbol{M} = \begin{bmatrix} \cos\alpha_{21} & \cos\alpha_{22} & -\sin\alpha_{23} & -\cos\alpha_{21} & -\cos\alpha_{22} & \sin\alpha_{23} \\ \sin\alpha_{21} & \sin\alpha_{22} & \cos\alpha_{23} & \sin\alpha_{21} & \sin\alpha_{22} & \cos\alpha_{23} \\ E_{21}k_{21} & E_{22}k_{22} & -G_{23}k_{23} & E_{21}k_{21} & E_{22}k_{22} & -G_{23}k_{23} \\ G_{21}k_{21} & G_{22}k_{22} & H_{23}k_{23} & -G_{21}k_{21} & -G_{22}k_{22} & -H_{23}k_{23} \\ S_{21} & S_{22} & -\bar{T}_{23} & -S_{21} & -S_{22} & \bar{T}_{23} \\ O_{21}k_{21} & O_{22}k_{22} & 0 & O_{21}k_{21} & O_{22}k_{22} & 0 \end{bmatrix}, \tag{8}$$

$$\boldsymbol{D_1} = \begin{bmatrix} \cos\alpha_{11} & -\cos\alpha_{11} & -\cos\alpha_{12} & \sin\alpha_{13} \\ \sin\alpha_{11} & \sin\alpha_{11} & \sin\alpha_{12} & \cos\alpha_{13} \\ E_{11}k_{11} & E_{11}k_{11} & E_{12}k_{12} & -G_{13}k_{13} \\ G_{11}k_{11} & -G_{11}k_{11} & -G_{12}k_{12} & -H_{13}k_{13} \\ S_{11} & -S_{11} & -S_{12} & \boldsymbol{T}_{13} \\ O_{11}k_{11} & O_{11}k_{11} & O_{12}k_{12} & 0 \end{bmatrix}, \tag{9}$$

$$\boldsymbol{D}_2 = \begin{bmatrix} W_{31}\cos\alpha_{31} & W_{32}\cos\alpha_{32} & -W_{32}\sin\alpha_{33} \\ W_{31}\sin\alpha_{31} & W_{32}\sin\alpha_{32} & W_{32}\cos\alpha_{33} \\ W_{31}E_{31}k_{31} & W_{32}E_{32}k_{32} & -W_{32}G_{33}k_{33} \\ W_{31}G_{31}k_{31} & W_{32}G_{32}k_{32} & W_{32}H_{33}k_{33} \\ W_{31}S_{31} & W_{32}S_{32} & -W_{32}\boldsymbol{T}_{33} \\ W_{31}O_{31}k_{31} & W_{32}O_{32}k_{32} & 0 \end{bmatrix}, \tag{10}$$

$$\boldsymbol{W}=\begin{bmatrix} W_{21} & 0 & 0 & 0 & 0 & 0 \\ 0 & W_{22} & 0 & 0 & 0 & 0 \\ 0 & 0 & W_{23} & 0 & 0 & 0 \\ 0 & 0 & 0 & W_{21}^{-1} & 0 & 0 \\ 0 & 0 & 0 & 0 & W_{22}^{-1} & 0 \\ 0 & 0 & 0 & 0 & 0 & W_{23}^{-1} \end{bmatrix}, \tag{11}$$

$$\boldsymbol{R_T}=\begin{bmatrix} 1 & \tilde{R}_{p1} & \tilde{R}_{p2} & \tilde{R}_{\mathrm{s}} & \tilde{T}_{p1} & \tilde{T}_{p2} & \tilde{T}_{\mathrm{s}} \end{bmatrix}^{\mathrm{T}}, \tag{12}$$

$$E_{lm}=A_l+2N_l\cos^2\alpha_{lm}+(Q_1+R_1)\,v_{lm}+Q_l, \tag{13}$$

$$G_{lm}=N_l\sin 2\alpha_{lm}, \tag{14}$$

$$H_{lm}=N_l\cos 2\alpha_{lm}, \tag{15}$$

$$S_{lm}=\phi_l\,(1-v_{lm})\cos\alpha_{lm}, \tag{16}$$

$$\bar{T}_{lm}=\phi_l\,(1-v_{lm})\sin\alpha_{lm}, \tag{17}$$

$$O_{lm}=\frac{Q_l+R_l v_{lm}}{\phi_l}, \tag{18}$$

$$W_{lm}=\mathrm{e}^{\mathrm{i}hk_{lm}\cos\alpha_{lm}}, \tag{19}$$

with k being the complex wave number, α the angle, A and N the elastic parameters of undrained skeleton, Q and R the elastic parameters related to the coupling of fluid and solid, v the ratio of the displacement of fluid to the displacement of solid, $l=1,2,3$ the subscripts referring to media I, II, and III, respectively, $m=1,2,3$ the subscripts referring to the FP-wave, SP-wave, and CS-wave, respectively, $\tilde{R}$ being the reflection coefficient, $\tilde{T}$ the transmission coefficient, $p1$, $p2$, and s the subscripts referring to the FP wave, SP wave, and CS wave, respectively.

In the matter of thin interbed, the equation of AVA response can be expressed by Eq. (20). The definition of $\boldsymbol{B}_j$ is the same as that of $\boldsymbol{B}$ and $\bar{J}$ is the number of the layers in the thin interbed.

$$\begin{bmatrix} \prod_{j=1}^{\bar{J}} \boldsymbol{B}_j\boldsymbol{D}_1 & -\boldsymbol{D}_2 \end{bmatrix}\boldsymbol{R_T}=0, \tag{20}$$

The seismic common depth point gather (CDP) in time domain can be obtained from the following equation:

$$\mathrm{Sig}\,(t,\alpha)=\mathrm{FFT}^{-1}\left[\tilde{R}\,(\omega,\alpha)\times\tilde{W}\,(\omega)\right], \tag{21}$$

where $\tilde{W}$ is the seismic wavelet, $\mathrm{Sig}(t,\alpha)$ the seismic CDP gather in time-incident angle domain.

Because the wave number in those equations above is complex number and frequency dependent, so in the equations considered are the frequency-dependent velocity and attenuation. And the structure of thin interbed is considered in Eq. (20).

4. FDAVA analyses of thin bed

The parameters of mudstone (medium I and medium III) are set to be the same value (Table 1), which will introduce small velocity dispersion and low attenuation. The parameters of sandstone (medium II) are set to be the values (Table 1) which will introduce high velocity dispersion and high attenuation in a range of seismic frequency (Fig. 2). The thin interbed is made up of alternating superposition of sandstone (medium II) and mudstone (medium I). In Table 1, G_{b} is shear modulus of skeleton and K_{b} is the bulk modulus of skeleton.

Table 1. Parameters of model based on BISQ model.

Parameters	ϕ/%	η/Pa·s	κ/mD	ρ_{f}/(kg/m^3)	ρ_{s}/(kg/m^3)	G_{b}/GPa	K_{b}/GPa	K_{s}/GPa	K_{f}/GPa	r/mm
Medium I	1	0.001	0.01	1000	2650	20	30	35	2.25	0.1
Medium II	30	0.03	1.25	900	2650	14.6	16	38	1.49	5

We use biconjugate gradient-stabilized method to solve linear equations (Eq. (6) or Eq. (20)).[39] The dispersion of FDAVA from 5-m-thin sandstone bed (Fig. 3(a)) is much higher and more complicated than that of thick layer (Fig. 3(b)). In the thick layer situation, the thickness of sandstone is much larger than the wavelength of seismic wave, and the reflection and transmission occur at the interface between mudstone and sandstone. The stack reflection amplitude of 0°–60° (which means adding the reflection coefficients with incident angle from 0° to 60°) from thick layer shows the property of low-frequency "bright spot" (Fig. 4(a)), but the stack reflection amplitude of 0°–60° of thin sandstone increases with frequency increasing (Fig. 4(b)). The difference between reflection coefficients of 10-Hz and 50-Hz waves from thin sandstone bed (Fig. 4(d)) is much higher than that from the thick layer (Fig. 4(c)). The CDP gather can be obtained by Eq. (21) and the wavelet is shown in Fig. 5. The low frequency component of CDP gather of thick layer (Fig. 6(a)) is much more obvious than that of the thin bed (Fig. 6(b)).

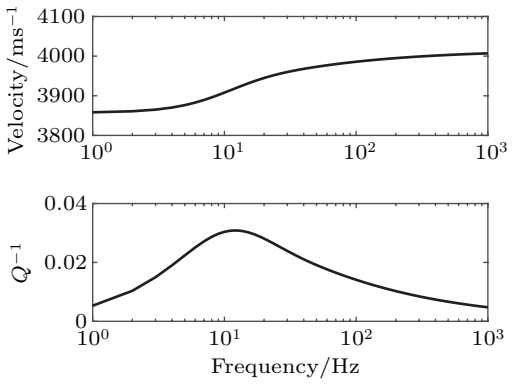


Fig. 2. Velocity and attenuation of FP wave *versus* frequency in sandstone.

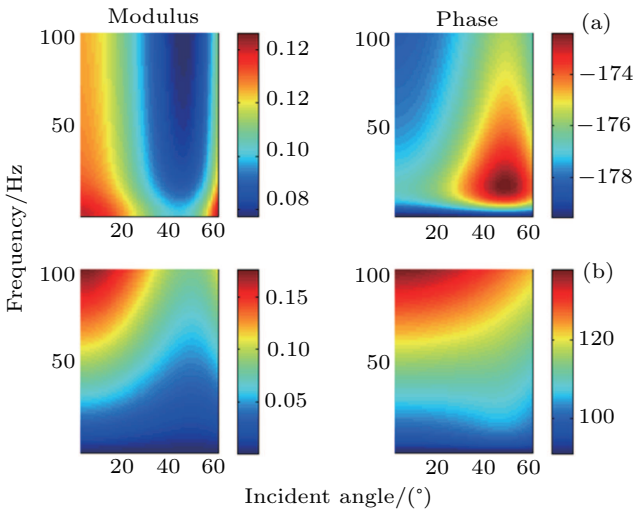


Fig. 3. FDAVA from (a) thick layer and (b) thin bed.

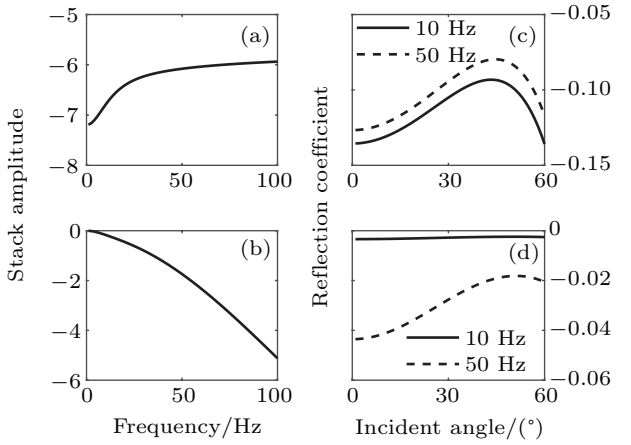


Fig. 4. Stack reflection amplitude *versus* frequency for (a) thick layer and (b) thin bed, and reflection coefficient *versus* incident angle for (c) thick layer and (d) thin bed.

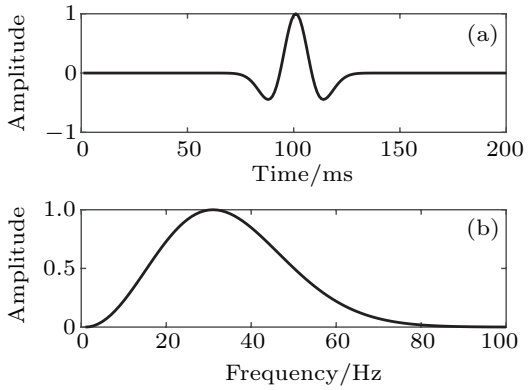


Fig. 5. Seismic wavelet in (a) time domain and (b) frequency domain.

The modulus and phase of reflection coefficient show the periodic characteristic in frequency domain (Fig. 7). That is because equation (19) involves the periodic phase term. The periodic property has the relationship between the thickness of thin bed and incident angle. So, it has the potential application prospect to obtain the thickness of the thin bed. The amplitude envelope of frequency-dependent coefficients in frequency domain decays according to exponential function of $e^{-2h\text{imag}(k_{21}(\omega))\cos\alpha_{21}}$ (Fig. 8).

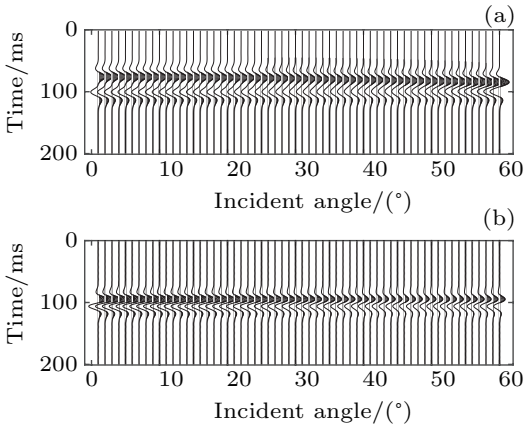


Fig. 6. CDP gathers of (a) thick layer and (b) thin sandstone bed.

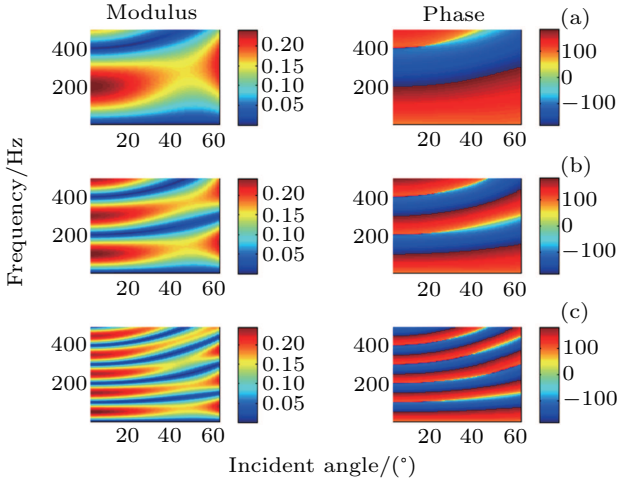


Fig. 7. Periodic FDAVA from thin bed with $h = 5$ m (a), 10 m (b), and 20 m (c), separately.

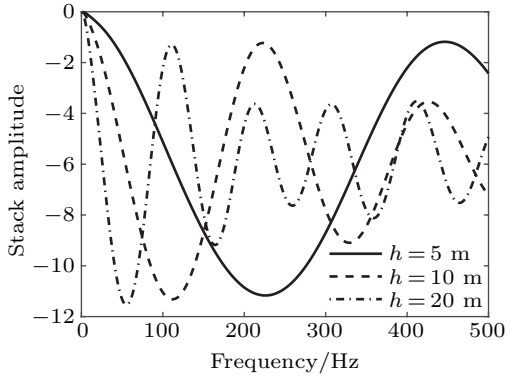


Fig. 8. Stack reflection amplitude of 0°–60° from thin bed with different thicknesses.

The reflection coefficient of 30-Hz wave increases with the thickness of thin bed increasing if the thickness is smaller than a quarter of wavelength. If the thickness is higher than a quarter of wavelength, the reflection coefficient decreases with thickness increasing when the incident angle is in a range of $0° \sim 40°$ (Fig. 9), and this incident angle range is important for seismic exploration.

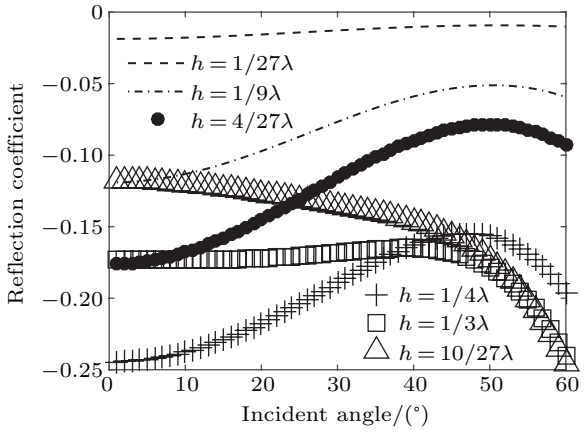


Fig. 9. Reflection of 30-Hz wave from thin bed with different thicknesses.

The general rules of FDAVA of thin interbed with fixed total thickness but different thicknesses of one layer ($\bar{h}$) in the interbed are basically consistent with each other (Fig. 10). The number of layers in interbed can be obtained from $\bar{J} = h/\bar{h}$. The stack reflection amplitude of 0°–60° (Fig. 11) and the reflection coefficient of 30 Hz (Fig. 12) wave increase slightly with the thickness of a layer in the interbed increasing.

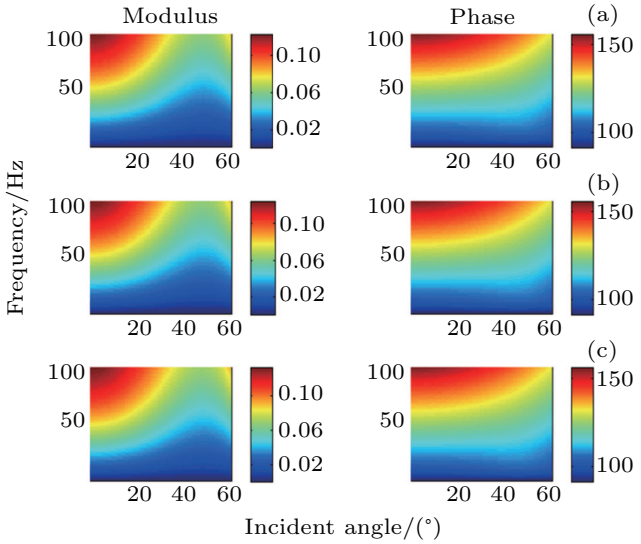


Fig. 10. FDAVA from thin interbed ($h = 7.5$ m) with $\bar{h} = 0.3$ m (a), 0.5 m (b), and 1.5 m (c), separately.

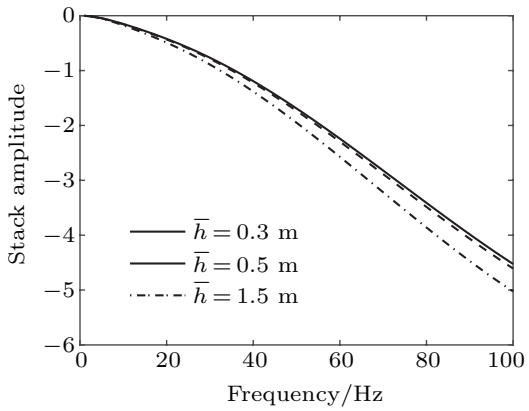


Fig. 11. Stack reflection amplitude of 0°–60° from thin interbed for $h = 7.5$ m.

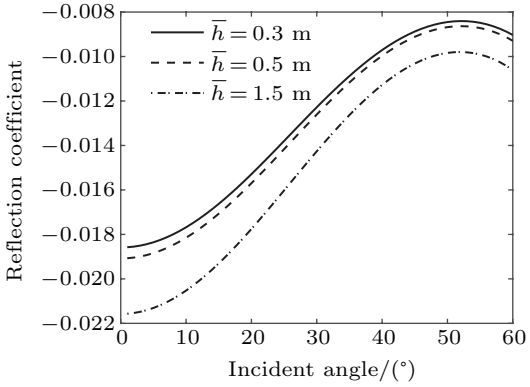


Fig. 12. Reflection coefficient of 30-Hz wave from thin interbed *versus* incident angle for $\bar{h} = 0.3$ m, 0.5 m, 1.5 m.

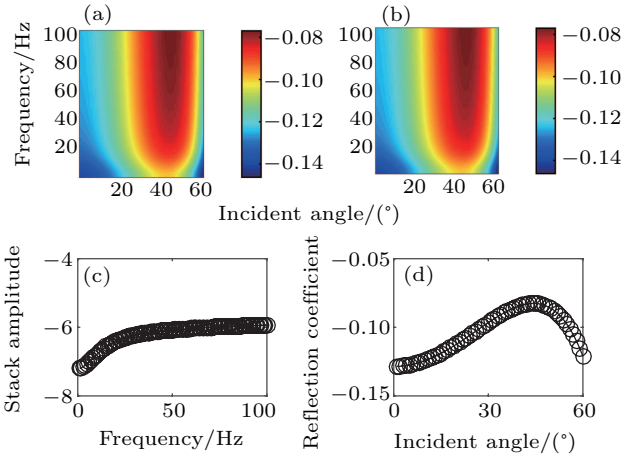


Fig. 13. FDAVA from thick layer with (a) and without (b) considering SP-wave, and (c) stack amplitude and (d) reflection coefficient of 30-Hz wave with (line) and without (circle) considering SP-wave.

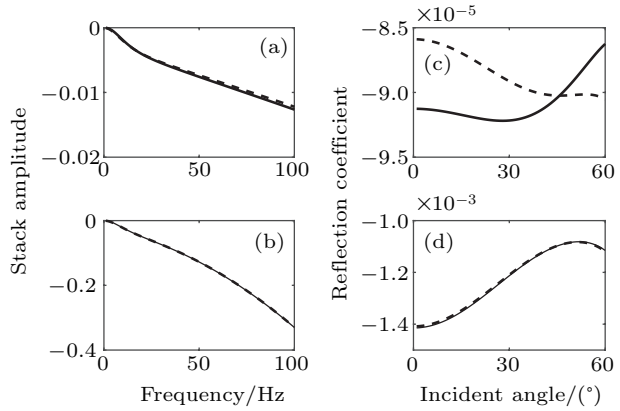


Fig. 14. Stack reflection amplitude from thin bed ($h = 0.1$ m (a) and 1 m (b)), and reflection coefficient of 30 Hz from thin bed ($h = 0.1$ m (c) and 1 m (d) with (broken line) and without (solid line) considering SP wave in boundary conditions.

There is SP wave in the porous media. The SP wave is difficult to receive in the seismic exploration work. That is caused by the high attenuation of SP wave. We compare the FDAVA of two types of thick layers: in the first type, the SP wave in the boundary condition is considered but in the second type the SP wave in the boundary condition is not considered. They are almost the same (Fig. 13). The stack reflection amplitude and AVA of 30-Hz wave of 0.1-m thin bed with considering the SP

wave in boundary condition are different from withthout considering the SP wave in boundary condition (Figs. 14(a) and 14(c)). But if the thickness of thin bed is 1 m, there is no obvious difference between them (Figs. 14(b) and 14(d)). That means the effect of SP wave on the AVA response cannot be ignored only if the thickness of thin bed is very small. So, in most conditions, the SP wave can be ignored in the boundary conditions.

5. Conclusions

The equations for calculating FDAVA from thin bed in porous media are obtained, with considering the effect of frequency-dependent velocity and attenuation, the thickness and structure of the thin bed. Through the numerical analysis, we obtain some conclusions below.

(i) The effect of SP wave on the FDAVA from thin bed in porous media can be ignored in most conditions except the fact that the thickness of thin bed is very small (cm level), which is likely to be caused by the high attenuation of SP wave, and the SP wave will decay in a short distance, which has been proved by the fact that it is difficult to detect slow P-wave in real survey.

(ii) The dispersion of FDAVA from the thin bed is much higher and more complicated than that from the thick layer, showing a periodic characteristic in frequency domain which is affected by the thickness of thin bed and incident angle. That is because the seismic wave dispersion of reservoir sandstone is much higher than that of surrounding mudstone. The envelope of stack reflection amplitude decays exponentially with frequency increasing, which is related to the thickness of thin bed, attenuation, and incident angle. So, it is possible to invert the thickness of thin layer by using the envelope of stack reflection amplitude changing with frequency. The stack reflection amplitude of FDAVA from the thick layer shows low frequency "bright spot", but the stack reflection amplitude of FDAVA from the thin bed increases with frequency increasing. This phenomenon can be used for thin reservoir to be identified.

(iii) The reflection coefficient increases with the thickness of the thin bed increasing if the thickness is smaller than a quarter of wavelength and then decreases when the thickness is higher than a quarter of wavelength. The general rules of FDAVA obtained from thin interbeds whose total thickness is the same but each layer thickness may be changed, are basically consistent with each other. This is because in the example in this paper, although the thickness of the single layer in the thin interbed is different, the ratio between the sand and mudstone is the same because they are alternately distributed with the same thickness.

References

[1] Meissner R and Meixner E 1969 *Geophys. Prospect.* **17** 1
[2] Widess M B 1973 *Geophysics* **38** 1176
[3] Kallweit R S 1982 *Geophysics* **47** 1035
[4] Chung H M and Lawton D C 1995 *Geophysics* **60** 223
[5] Liu Y and Schmitt D R 2003 *Geophysics* **68** 1161
[6] Yang C, Wang Y and Wang Y H 2016 *Geophysics* **81** N31
[7] Lu Y F and Han Y P 2019 *Chin. Phys. B* **28** 024202
[8] Gassmann F 1951 *Geophysics* **16** 673
[9] Biot M A 1956 *J. Acoust. Soc. Am.* **28** 168
[10] Biot M A 1956 *J. Acoust. Soc. Am.* **28** 179
[11] Biot M A 1962 *J. Acoust. Soc. Am.* **34** 1254
[12] Biot M A 1968 *J. Acoust. Soc. Am.* **44** 1616
[13] Mavko G and Nur A 1975 *J. Geophys. Res.* **80** 1444
[14] Mavko G and Nur A 1979 *Geophysics* **44** 161
[15] White J E 1975 *Geophysics* **40** 224
[16] Dvorkin J and Nur A 1993 *Geophysics* **58** 524
[17] Johnson D L 2001 *J. Acoust. Soc. Am.* **110** 682
[18] Berryman J G and Wang H F 2000 *Int. J. Mech. Min.* **37** 63
[19] Pride S R, Berryman J G and Harris J M 2004 *J. Geophys. Res.: Solid Earth* **109** 1
[20] Tao C H, Li H X, Deng X M, Zhou J P, Fu S S, Wilkens R H, Gu C H and He Y H 2010 *Chin. Ocean Eng.* **24** 381
[21] Ba J, Carcione J M, Cao H, Du Q Z, Yuan Z Y and Lu M H 2012 *Chin. J. Geophys.* **55** 219 (in Chinese)
[22] Spano T J T 2009 *Transp. Porous Med.* **79** 135
[23] Chichinina T I, Obolentseva I R and Ronquillo J G 2009 *Transp. Porous Med.* **79** 1
[24] Li H X, Tao C H, Goloshubin G, Liu C, Shi S H, Huang G N, Zhang H, Zhang J and Zhang X F 2018 *Phys. Acoust.* **64** 453
[25] Qiu H M, Xia T D, He S H and Chen W Y 2018 *Acta Phys. Sin.* **67** 204302 (in Chinese)
[26] Silin D B and Goloshubin G M 2010 *Transp. Porous. Med.* **83** 233
[27] Arora A and Tomar S K 2010 *Transp. Porous Med.* **85** 375
[28] Carcione J M, Morency C and Santos J E 2010 *Geophysics* **75** 229
[29] Li H X, Gui L F, Tao C H and Liu C 2015 *Acta Petrolei. Sin.* **36** 1108 (in Chinese)
[30] Li H X, Tao C H, Liu C, Goloshubin G, Huang G N, Zhang H, Shi S H, Zhang J and Zhang X F 2019 *J. Porous Media* **22** 435
[31] Wang T, Zheng K C, Jia Y P, Fu C L, Gong Z J and Wu W F 2017 *Chin. Phys. B* **26** 074701
[32] Chapman M, Liu R and Li X Y 2005 *Leading Edge* **24** 1120
[33] Chapman M, Liu E R and Li X Y 2006 *Geophys. J. Int.* **167** 89
[34] Ren H T, Goloshubin G and Hilterman F J 2009 *Geophysics* **74** N41
[35] Silin D B, Korneev V A, Goloshubin G M and Patzek T W 2006 *Transp. Porous Med.* **62** 283
[36] Quinta B 2012 *J. Appl. Geophys.* **82** 119
[37] Chabyshova E and Goloshubin G M 2014 *Geophysics* **79** 417
[38] Guo Z Q, Liu C, Li X Y and Lan H T 2016 *Chin. J. Geophys.* **59** 664 (in Chinese)
[39] Zhang Y, Wang H N, Tao H G and Yang S W 2012 *Chin. J. Geophys.* **55** 2141 (in Chinese)